ELSEVIER

Journal of Neuroscience Methods 94 (1999) 121–140

JOURNAL OF NEUROSCIENCE METHODS

www.elsevier.com/locate/jneumeth

Principal component analysis of neuronal ensemble activity reveals multidimensional somatosensory representations

John K. Chapin [a,*], Miguel A.L. Nicolelis [b]

[a] *Department of Neurobiology and Anatomy, MCP Hahnemann University, 3200 Henry Ave., Philadelphia, PA 19129, USA*
[b] *Department of Neurobiology, Duke University Medical Center, Box 3209, Durham, NC 27710, USA*

Received 25 July 1999; accepted 9 August 1999

Abstract

Principal components analysis (PCA) was used to define the linearly dependent factors underlying sensory information processing in the vibrissal sensory area of the ventral posterior medial (VPM) thalamus in eight awake rats. Ensembles of up to 23 single neurons were simultaneously recorded in this area, either during long periods of spontaneous behavior (including exploratory whisking) or controlled deflection of single whiskers. PCA rotated the matrices of correlation between these *n* neurons into a series of *n* uncorrelated principal components (PCs), each successive PC oriented to explain a maximum of the remaining variance. The fact that this transformation is mathematically equivalent to the general Hebb algorithm in linear neural networks provided a major rationale for performing it here on data from real neuronal ensembles. Typically, most information correlated across neurons in the ensemble was concentrated within the first 3–8 PCs. Each of these was found to encode distinct, and highly significant informational factors. These factor encodings were assessed in two ways, each making use of fact that each PC consisted of a matrix of weightings, one for each neuron. First, the neurons were rank ordered according to the locations of the central whiskers in their receptive fields, allowing their weightings within different PCs to be viewed as a function of their position within the whisker representation in the VPM. Each PC was found to define a distinctly different topographic mapping of the cutaneous surface. Next, the PCs were used to weight-sum the neurons' simultaneous activities to create population vectors (PVs). Each PV consisted of a single continuous time series which represented the expression of each PC's 'magnitude' in response to stimulation of different whiskers, or during behavioral events such as active tactile whisking. These showed that each PC functioned as a feature detector capable of selectively predicting significant sensory or behavioral events with far greater statistical reliability than could any single neuron. The encoding characteristics of the first few PCs were remarkably consistent across all animals and experimental conditions, including both spontaneous exploration and direct sensory stimulation: PC1 positively weighted all neurons, mainly according to their covariance. Thus it encoded global magnitude of ensemble activity, caused either by combined sensory inputs or intrinsic network activity, such as spontaneous oscillations. PC2 encoded spatial position contrast, generally in the rostrocaudal dimension, across the whole cutaneous surface represented by the ensemble. PC3 more selectively encoded contrast in an orthogonal (usually dorsoventral) dimension. A variable number of higher numbered PCs encoded local position contrast within one or more smaller regions of the cutaneous surface. The remaining PCs typically explained residual 'noise', i.e. the uncorrelated variance that constituted a major part of each neuron's activity. Differences in behavioral or sensory experience produced relatively little in the PC weighting patterns but often changed the variance they explained (eigenvalues) enough to alter their ordering. These results argue that PCA provides a powerful set of tools for selectively measuring neural ensemble activity within multiple functionally significant 'dimensions' of information processing. As such, it redefines the 'neuron' as an entity which contributes portions of its variance to processing not one, but several tasks.

Keywords: Principal components analysis; Neuronal ensemble activity; Sensory information processing; Neuron

1. Introduction

One of the central concepts of contemporary neuroscience is that major brain functions are executed

* Corresponding author.

0165-0270/99/$ - see front matter
PII: S0165-0270(99)00130-2

through the joint actions of ensembles of neurons (Erickson, 1968; Churchland, 1989). This mode of computation may have similarities to parallel distributed processing (PDP; Rumelhart et al., 1986a), in which information is not localized within individual neurons, but instead is distributed across neuronal populations. Thus, no single neuron is necessary for any one computation, yet each neuron can participate in a large number of computations. Computations involve resolving information embedded in patterns of correlated activity among large populations of afferent inputs.

Assuming that such distributed processing occurs in real neuronal populations, how might it be studied? According to theory, information which is distributed across a neuronal ensemble should be manifested as patterns of correlated activity among the neurons. Unfortunately, it is very difficult to resolve the underlying structure of information contained within large numbers of pairwise correlations between simultaneously recorded neurons. As an alternative, this paper examines the use principal components analysis (PCA) for analysis of real distributed neuronal networks. PCA is a classical technique for obtaining an optimal overall mapping of linearly dependent patterns of correlation between variables (e.g. neurons). PCA provides, in the mean-squared error sense, an optimal linear mapping of the 'signals' which are spread across a group of variables. These signals are concentrated into the first few components, while the 'noise', i.e. variance which is uncorrelated across variables, is sequestered in the remaining components. PCA has been used extensively to resolve temporal patterns in neurophysiological recordings (McClurkin et al., 1991; Kjaer et al., 1994). Here, PCA was used to map the neuronal ensemble information in up to 23 simultaneously recorded neurons in the vibrissa-sensory region of the ventral posterior medial (VPM) thalamus of awake rats, during spontaneous behaviors (including exploratory whisking) and controlled deflection of single whiskers.

A further rationale for using PCA to map patterns of neuronal correlation is that it is known to be mathematically equivalent to the general Hebb algorithm for learning in linear neural networks (Oja, 1982, 1989, 1992; Bourlard and Kamp, 1988; Baldi and Hornik, 1989; Sanger, 1989; Hertz et al., 1991; Hrycej, 1992). Most self organizing artificial neural network models utilize some variant of Hebbian learning, in which synaptic strengths are modified according to the temporal correlation of the synaptic inputs with post-synaptic neuronal activation. Since post-synaptic activation is normally caused by increased synaptic input, the Hebb rule increases synaptic strengths according to their temporal correlation with other inputs.

The ultimate aim of this study was to record activity of neuronal ensembles at the thalamic level of the somatosensory system, and then to use PCA to evaluate the mapping of sensory information, providing clues as to how thalamic signals are transformed in their transmission through the cortical circuitry. For this purpose it was necessary to obtain recordings of neuronal activity during long periods of spontaneous behavior, hopefully to obtain a representative sample of the normal repertoire of information handled by these neurons. While several investigators have demonstrated that experience dependent factors can influence patterns of sensory mapping in the neocortex, no study has yet employed actual simultaneous recordings to evaluate how the sensory information might be transformed by Hebb-like learning. For this purpose, PCA is advantageous in that it provides a mathematically well understood technique for mapping the informational factors comprising linearly dependent patterns of covariance in a neuronal ensemble. On the other hand, independent components analysis (ICA) is more appropriate for identification of nonlinear and/or independent patterns of covariance (Laubach et al., 1999).

2. Materials and methods

2.1. Recording procedures

Complete methods for the simultaneous many-neuron recording techniques are discussed in detail elsewhere (Shin and Chapin, 1990; Nicolelis et al., 1993, 1995; Nicolelis and Chapin, 1994). Briefly, a multi-channel unit recording/discrimination system (Plexon Inc, Dallas, TX) single neuron action potentials were recorded through arrays of 16 microwire electrodes (25 or 50 μm diameter, Teflon insulated stainless steel; NB Labs, Dennison, TX) implanted across the whisker representation in the VPM in Long–Evans (Hooded) rats. Recording experiments commenced approximately 1 week following surgery. Once in the recording chamber, a wiring harness was plugged onto the previously implanted headstage. The multi-neuron recording system allowed simultaneous amplification, bandpass filtering, window discrimination and computer storage of spike-times from large numbers of single neurons. Approximately 90% of the microwire electrodes yielded at least one discriminable waveform (signal/noise ratio at least 5). Online single unit discrimination used digital signal processors (DSPs) incorporating both voltage–time window and principal component clustering waveform discrimination algorithms. The sample experimental data sets utilized here included up to 23 neurons recorded simultaneously in the VPM thalamus.

Receptive fields (RFs) were quantitatively characterized by mechanically displacing single whiskers using a computer controlled vibromechanical actuator. Eight to 20 different facial whiskers were stimulated 300–600 times apiece (3° deflections, 0.1 s step pulses, delivered at 1 Hz), yielding a highly quantitative data base for

evaluation of these neurons' sensory properties. Such data obtained from the same neurons under awake and/or anesthetized conditions yielded a center RF for each neuron. After the awake animals were highly habituated to the whisker stimulation procedure they rested quietly without moving.

Recordings were also obtained during 20- to 60-min periods of spontaneous behavior, which included episodes of rest, exploratory whisking, grooming and locomotion. During recordings in awake, freely moving animals, the rat's behavior was continuously monitored and stored on video tape. A Lafayette Super-VHS video analysis system was used for field-frame analysis of these video tapes (1/60th s resolution). Synchronization of the videotape with experimental recording data was achieved by using a 100 Hz output from the data acquisition computer (Motorola VME delta system) to update a Thalner video counter-timer (Ann Arbor, MI), which produced a time-stamp with 10 ms resolution, displayed on each fieldframe.

Analysis of recorded data, including the PCA algorithm described below, was carried out using software developed by JKC to run on a Motorola VME delta system. Further statistical and graphical analyses were carried out using the CSS-Statistica package (Tulsa, OK) on principal components (PCs).

2.2. Statistical techniques

2.2.1. Covariance, cross-correlation and cross-correlograms

Single neuron discharge was quantized by integrating over time bins ranging from 5 to 500 ms (with 10 ms as a standard). For statistical analysis, each neuron constituted a 'variable', and its spike count for each bin (generally over the whole experiment) was a 'sample'. First, correlation or covariance matrices were calculated. Statistical significance of these correlation coefficients was calculated by the formula,

$$r = tS_{\mathrm{r}}$$

where t is Student's t-test, and

$$S_{\mathrm{r}}\sqrt{\frac{1-r^2}{(n-2)}}$$

where n is the number of data samples.

2.2.2. Principal components analysis (PCA)

The theory of principal components states that every symmetrical covariance or correlation matrix relating p random variables $X1$, $X2,\ldots,Xn$ can be transformed into particular linear combinations by rotating the matrix into a new coordinate system. This rotation is produced by multiplying each of the original data variables by their appropriate weighting coefficients. For each component, these weights comprise a vector called an eigenvector, and the variance 'explained' by its eigenvalue. The original matrix is rotated such that the axis defined by the first principal component (PC1) is aligned in the direction of greatest variance, hence maximizing the eigenvalue. To obtain the second component (PC2) the matrix is rotated around the PC1 axis to obtain a second eigenvector which again contains the greatest possible amount of remaining variance. This procedure is repeated until a set of N orthogonal (uncorrelated) components is obtained, arranged in descending order of variance. In this transformation, none of the information contained within the original variables is lost, and the derived components can be statistically manipulated in the same way as the original variables. Moreover, the transformation is useful because most of the significant total variance (i.e. correlated neuronal information) is concentrated within the first few uncorrelated PCs, while the remaining PCs mainly contain 'noise' (i.e. uncorrelated neuronal information). The first few PCs not only provide a simpler and more parsimonious description of the covariance structure, they also concentrate the information which is normally spread across multiple variables (neurons) into a single, more statistically useful 'factor'.

The squares of these weighting coefficients represent the correlations of each variable (neuron) with the PC. Since each component is apportioned some fraction of the total variance of the neuron, the sum of squared coefficients across each row must equal 1.0. A further constraint is that the sums of squared coefficients for each component must also equal 1.0. Thus the total variance contained in the ensemble can be represented either in terms of the combination of neurons (i.e. across rows in the eigenvector matrix), or the combination of principal components (i.e. across columns).

2.2.3. Characterization of statistical error

Although PCA is a distribution free method it is sometimes useful to assess the statistical significance of the eigenvalues and principal component coefficients obtained. The following formulas were used here for calculation of S.E. of eigenvalues,

$$s(\lambda) = \lambda_h \times \sqrt{\frac{2}{n-1}} \tag{4}$$

and principal component coefficients:

$$s(b_{hj}) = \sqrt{\left[(1/n-1)\lambda_h\left(\sum_{k=1}^{p}\lambda_k/(\lambda_{k-1}h)^2(b_{kj}^2)\right)\right]} \tag{5}$$

where n is the number of samples, λ_h is the eigenvalue of component h, b_{hj} is the jth coefficient of the hth component, and p is the total number of components.

These formulae apply to principal components analyses carried out on covariance matrices. However, since correlation matrices are equivalent to covariance matrices calculated from standardized data, the S.E. can

be considered appropriate when standardized data are used to construct a covariance matrix. These formulas are technically correct except when used for data with small numbers of samples and for severely non-Gaussian distributed data. The typical situation for the simultaneous neural recordings here is to obtain a very large (10^3 to 2×10^5) number of samples, with near-Poisson distributed data. As shown in Fig. 1, these data converge on normality with increasing sample integration times.

2.2.4. Interpretation of PCA results

Since PCA involves successive rotations of a covariance matrix, the configuration of each derived PC is a function of the previous (lower numbered) PCs. Thus, the PCs may not each represent a single factor underlying the population covariance, but instead may provide rules for separating between such factors. PCA is not, therefore, the method of choice for separating between completely independent factors, but is an excellent technique for defining a multidimensional mapping scheme for linear representation of a set of interdependent factors. As such, PCA should be ideal for analyzing processing of sensory information which normally involves interdependent factors, such as movements of stimuli over continuous receptor surfaces.

2.2.5. Using PCA to construct eigenfunctions

After their derivation here, the PCs were then used to create eigenfunctions by using the PC weights to

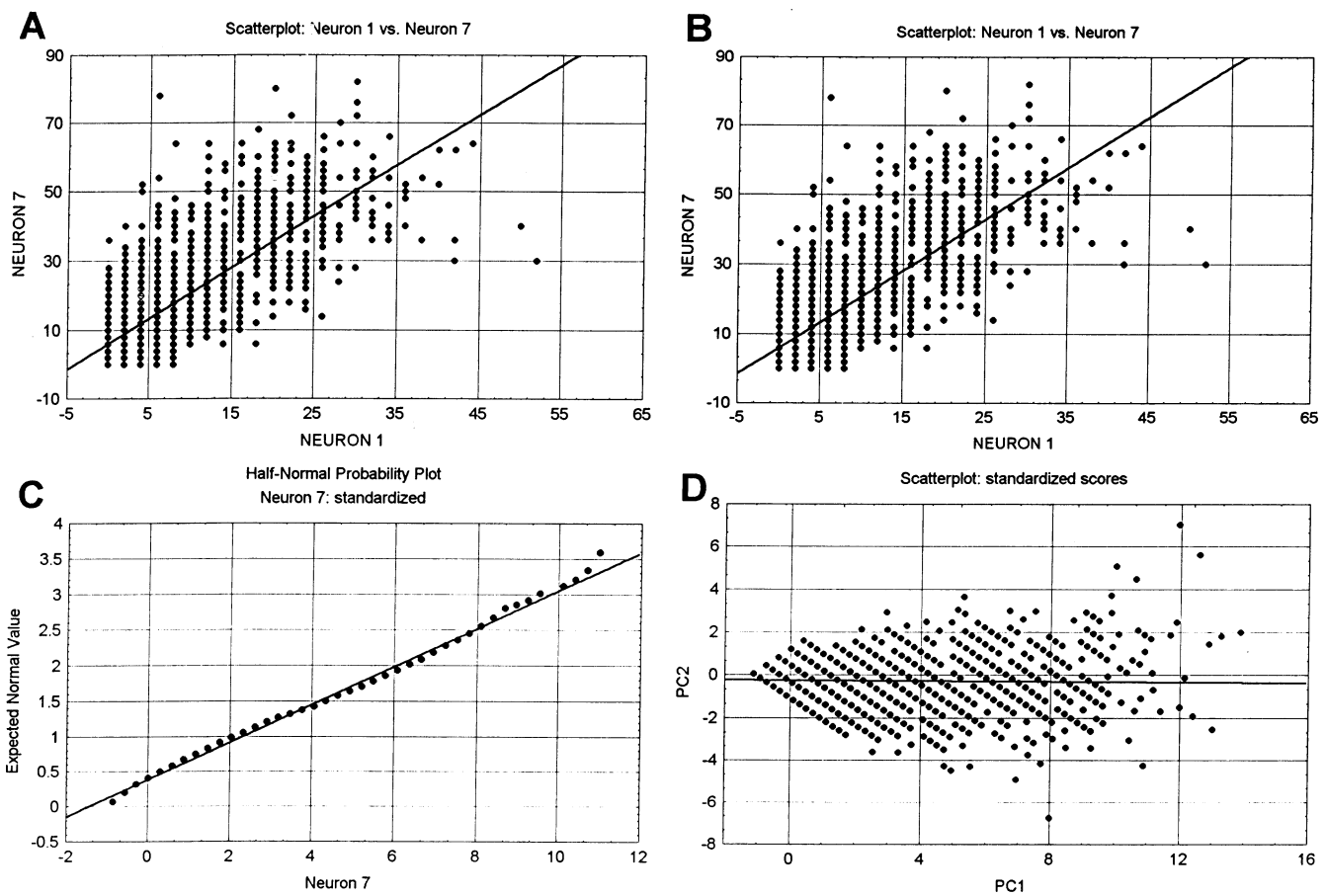

Fig. 1. Eigenvalue rotation of a two-neuron cluster plot. (A) Scatterplot showing the distribution of joint activity states in an ensemble of two neurons (1 and 7) recorded simultaneously in the PrV nucleus. (Both of these were among 47 recorded across multiple levels of the somatosensory system.) The position of each point depicts the firing rates of these two neurons over a single 500-ms time interval in a continuous experiment lasting 1800 s. The line through this point cluster shows their linear regression. Their correlation coefficient is 0.61 ($P \ll 0.01$). Since the coordinates of these points are integers, many overlap. (B) Scatterplot showing the same data after standardization by subtracting the mean and then dividing by the S.D. This removes excessive biasing of neurons with higher firing rates. (C) Half-normal probability plot showing that integrated spiking data converges on a normal distribution. The solid line shows the expected distribution of points in a perfectly normal (Gaussian) distribution. Points show the standardized scores from neuron 7 which were used to construct Fig. 3B. (D) Scatterplot shows the same data from neurons 1 and 7 after axis rotation using PCA. The best linear fit through the original points shown by the regression line in Fig. 1B is now oriented perfectly along (i.e. is 'explained' by) the first principal component (PC1), with the second principal component explaining the 'noise' in the perpendicular axis. The coordinates of the points in this new space defined by components 1 and 2 were calculated as weighted sums (i.e. the dot product) of the original standardized scores (from Fig. 1B). See text for principal component weights used to achieve this rotation.

weight-sum the time integrated data stream from each of the original neurons. Each eigenfunction is therefore a continuous time series containing an analog value for each time bin within the experiment. Typically, these time bins are chosen to be the same as the time integrals used to calculate the original correlation matrix used for the PCA. As shown in the equation below, each point Y_{pt} in an eigenfunction is defined as the linear combination of the standardized, time integrated spike counts recorded during that time bin from the original neurons, X_{pt} multiplied by the appropriate eigenvector weights Bp.

$$Y_1 = e'_1X = e_{11}X_1 + e_{21}X_2 + \ldots e_{p1}X_p$$

$$Y_2 = e'_1X = e_{12}X_1 + e_{22}X_2 + \ldots e_{p2}X_p$$

$$Y_p = e'_1X = e_{1p}X_1 + e_{2p}X_2 + \ldots e_{pp}X_p$$

where $e'i$ are eigenvectors, and e_{ij} are eigenvector weightings.

In this case X_i is the spike count of neuron i within a particular time bin. Though Y_p is commonly weighted by the eigenvalue λ, this is unnecessary for our applications. Also, when correlation matrices are used as input for the PCA it is necessary to first standardize X_i by subtracting the mean and dividing by the S.D. The eigenfunctions constructed using this technique constitute composite variables which, in statistical terms, can be treated much like the original variables (neurons). Since they are constructed from summations of weighted and standardized data, the eigenfunction magnitudes can be thought of in terms of 'population' firing rates, with units in Hz, but unrelated to actual firing rates of single neurons. In the figures below, eigenfunctions are used like traditional neurophysiological data, in stripcharts and peri-event averages.

3. Results

3.1. Data sets

This investigation utilized data obtained from a series of experiments in which ensembles of single neurons were simultaneously recorded through microwire electrode arrays implanted at different levels of the trigeminal somatosensory system in awake Long–Evans (Hooded) rats. A total of 707 neurons were recorded at various levels of the trigeminal somatosensory system in 20 rats during 497 different recording experiments ranging from 5 to 60 min in duration. Of these, 481 neurons were recorded in the ventral posteromedial (VPM) thalamic nucleus, specifically in the subregion which represents the mystacial whiskers. Of these, 127 VPM thalamic neurons in eight animals (ranging from eight to 24 neurons/animal) were recorded under experimental conditions meeting acceptable criteria for inclusion in this study. These conditions required that at least eight well discriminated single neurons be simultaneously recorded in the VPM thalamus of an awake rat over at least one 20- to 40-min period of spontaneous exploratory whisking behavior, and also over a number of discrete whisker stimulation experiments sufficient to quantitatively define the RFs of each neuron.

These animals were typically first recorded during a long period of spontaneous exploratory behavior in which the animal used its whiskers to explore objects in the experimental chamber. Post-hoc analyses of synchronized videotape records of this behavior typically show that rats spend about 50% of their time engaging in spontaneous whisking movements, especially including active sweeping of the mystacial whiskers tactile objects. In subsequent experiments under awake and anesthetized conditions the RF properties of the same neurons were quantitatively measured using a computer-controlled vibromechanical actuator to repetitively displace single whiskers or multi-whisker bundles. Thus, these experiments measured the responses of trigeminal somatosensory system neuronal ensembles to sensory stimulation either delivered passively to single whiskers or obtained actively through exploratory movement of the same whiskers over objects. The data sets were thus ideal for defining neuronal population information (using eigenfunctions) within somatosensory neuronal ensembles in the context of active tactile exploration.

3.2. Example of analysis

In a typical experimental protocol, spiking data from 23 well discriminated VPM neurons were simultaneously recorded over a single experimental day. First, the RFs of each neuron (i.e. their principal whiskers) were defined by aural monitoring of unit activity. Next, the 23 neurons were recorded during a 1821.49 s period of spontaneous behavior that included several long episodes of exploratory whisking. Subsequently, nine 5- to 15-min experiments were conducted to measure the same neurons' responses to controlled vibromechanical stimulation of each of nine single whiskers.

In post-hoc analysis, a correlation matrix between these 23 neurons was first calculated from the data recorded during the spontaneous exploratory period. This matrix revealed positive correlation coefficients (r) ranging from 0.0054 to 0.39. Despite the relatively low r values, they are highly statistically significant (S.E.M. 0.00354) because of the large number of samples (72 859, using 25-ms time integrals). Thus $r > 0.011$ was the confidence limit for a correlation significance at the $P < 0.001$ confidence level. In this matrix of 242 ($(n-1)2'_2$) correlation pairs, all but one r exceeded zero by at least this confidence limit. Moreover, the average r in this matrix was 0.137, i.e. 12.45 times the confidence limit.

3.3. Using PCA to map covariance structure

The 'eigenvalue decomposition' utilized by PCA involves rotating the covariance matrix to define a new set of orthogonal axes oriented in directions of greatest covariance. As shown in Fig. 1, this can be visualized as a rotation of a scatterplot in N-dimensional space in which each point defines the state of an N-neuron ensemble within a particular time interval. To illustrate, Fig. 1A shows a 2D scatterplot which depicts the correlation between the time integrated activities of two simultaneously recorded neurons in the VPM (unit 1 vs unit 7). Fig. 1A was constructed by quantizing the 1821 s experiment into 3642 bins (using 500-ms time integrals for illustration purposes). The spike counts of the two neurons within each bin are plotted as a point (vector) in an $X-Y$ space, such that the point's position represents the 'functional state' of the two-neuron ensemble. The r-value of these neuron's correlation was 0.61, which is highly significant ($P \ll 0.001$). This high positive correlation can be visualized by the preponderance of points lying along the 45° line in Fig. 1A.

Though PCA can utilize either covariance or correlation matrices, use of the former was discontinued because the PCA results tended to be dominated by the variance of a few rapidly firing neurons. To more accurately measure the co-activity of different neurons, this study utilized correlations, which are equivalent to covariances between standardized variables. Fig. 1B shows the scatterplot in Fig. 1A after standardization. Standardization of neuronal discharge rates (by subtracting the mean and dividing by the S.D.) normalized the activity rates of all neurons to 0.0, and their variances to 1.0. Even though PCA is a distribution free method for transformation of multivariate data, inferences about the statistical significance of eigenvalues and eigenvector coefficients are based on normally distributed data. Though we have found that integrated spike-train data tend to approximate Poisson or super-Poisson distributions, they tend to converge on a normal (Gaussian) distribution as they are integrated over longer time periods (demonstrated in Fig. 1C) or larger populations. Thus, the issue of data distribution can be handled in several ways. First, large numbers of data samples are used. Most parametric statistical techniques are quite robust against distribution anomalies when n is large (e.g. over 100). Second, Poisson distributed integrated spike train data converge on a normal distribution when larger integration times are used, or when large numbers of neurons are integrated into an eigenfunction. Finally, one can utilize square-root transformations to force Poisson distributed data into a more normal distribution. We have used such transformations routinely but have not found the results to be substantially different from analyses using untransformed data.

3.4. Calculation of principal components

Fig. 1D illustrates the use of PCA to rotate the scatterplot in Fig. 1B, which itself was constructed by standardizing the data in Fig. 1A. The rotation of the 3D scatterplot was produced by using PCA-derived coefficients for each component (PC1: 0.707 for both neurons; PC2: 0.707 and -0.707 for neurons 2 and 7, respectively). The set of coefficients for each PC defines a rotation vector (eigenvector) which, by dot product multiplication of the coordinates of the points in Fig. 1B, produced the scatterplot in Fig. 1D. This counterclockwise rotation produced a new X-axis (now called PC1) which is aligned along the long axis of the scatterplot. The position of a point along this new axis now constitutes an optimal measure of whatever factor(s) were originally responsible for producing the correlated discharge between the neurons.

The eigenvalues, representing the percentage of the total variance explained by each of these principal components were calculated as 70.13 for PC1, and 29.87 for PC2. PC1 can be considered as a mathematical definition of a new coordinate system which parallels the major factor of interaction between these neurons, defined purely in terms of their correlation in this data set. PC2, which must be orthogonal to component 1, accounts for the remainder of the variance, which may represent noise, or a less significant factor of interaction between the variables.

3.5. Using PCA to map functional relationships within neuronal ensembles

Distinct, functionally significant patterns of PC weightings emerged when the above techniques were applied to data from larger neuronal ensembles. Fig. 2 illustrates the PC weightings obtained through analysis of the 23-neuron data set discussed above. To investigate the relationship between these weightings and the topographic representation of whiskers in the VPM, each neuron was graphically rank ordered according to the rostrocaudal position of its RF center, i.e. its principal whisker, an accurate indicator of its actual position in the VPM. This provided visualization of the spatial attributes of the PC weighting patterns, allowing them to be interpreted rather like a receptive field (RF).

Fig. 2A provides a good example of the multi-topographical patterns found in PC weightings throughout this study. PC1 (top) invariably contained relatively homogeneous, all positive weightings, and was therefore essentially non-topographical. As such, PC1 primarily encoded the magnitude of global activity in this ensemble: the neurons most weakly weighted in this PC were found to be those which had very weak responses to sensory stimuli. Neurons 21–23 (from left) exhibited no clear RFs, and neurons 6 and 8–10 exhibited very

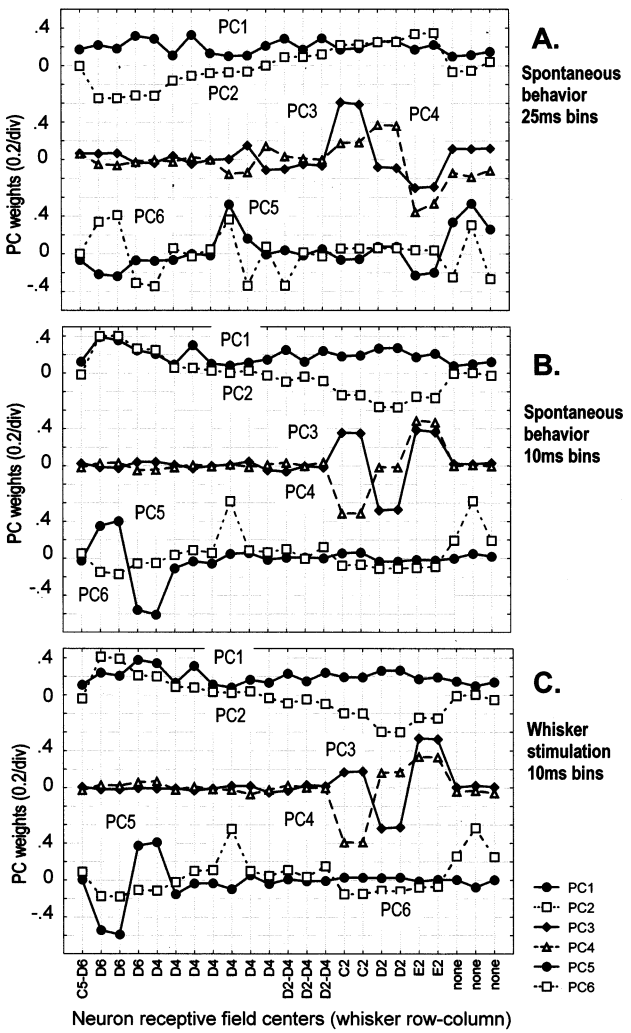

Fig. 2. Weighting coefficients of principal components derived from the same set of 23 neurons are similar over different experimental paradigms. (A) Linear graphs depicting weighting coefficients of principal components (PCs) 1–6 calculated from simultaneous recordings of 23 neurons in the VPM thalamus during an 1821.49 s sequence of spontaneous behavior in an awake rat. The 23 neurons are rank ordered on the *X*-axis according to the rostrocaudal locations of the centers of their RFs on the mystacial whiskers. The RF centers were quantitatively determined using peri-whisker-stimulation histograms. The mystacial whiskers in rat are commonly divided into rows A–E (dorsal-ventral), and columns 1–7 (caudal-rostral). The much smaller guard hairs (GH) are rostral to the mystacial whiskers. When more than one neuron was centered on the same whisker (e.g. the three neurons on D6) they were rank ordered according to the value of their coefficients in PC2. Three neurons did not have RFs on the whiskers (labeled 'N'). (B) Similar linear graphs depicting principal components derived from recordings of the same neurons in an experiment (20 min after that in (A)). For most of this experiment the animal remained still, allowing whisker E2 to be deflected using a computer controlled hand-held vibromechanical stimulator. The *X*-axis contains the same rank ordering of neurons as in (A). Note that the PCs are similar to those in (A), but are reversed in polarity and changed in order (e.g. PC3 and PC4 here are reversed in polarity and order compared to (A)).

weak sensory responses even though they had RFs centered on whisker D4. In contrast, PC2 almost linearly encoded the neurons according to the rostrocaudal position of their principal whiskers on the face. (The D6 whisker was weighted most negatively; the E2 whisker most positively.) To a lesser extent, PC3 encoded dorsoventral position, positively weighting the two neurons with RFs in the caudal C-row (both covering C2, but also extending to the D-row), and negatively weighting the two neurons with RFs in the E row.

Regression analysis was used to statistically validate this observation that PCs 2 and 3 defined gradients across the whisker pad. The weights for PCs 1–4 (dependent variables) were regressed against the spatial positions of the neurons' RF centers (independent variables). These RF centers were defined either in vertical coordinates (whisker rows A– E, numbered 1–5) or horizontal coordinates (whisker columns 1–6, and guardhairs = 7). When the RF centers covered multiple whiskers, the midpoint between them was used. The three neurons without RFs were omitted. When PCs 1–4 were regressed against the neurons' column number, PC2 yielded a coefficient of determination (R^2) of 0.69 ($F = 41.4$; $P = 5 \times 10^{-6}$), while the R^2s of the other PCs were insignificant (PC1: 0.006, PC3: 0.009, PC4: 0.0003). Thus, the rostrocaudal positions of center RFs on the whisker pad were robustly and selectively encoded by PC2. Similarly, dorsoventral position was selectively encoded by PC3, even though this sample contained relatively few cells with RFs in the C and E rows: When regressed against row number, PC3 yielded an R^2 of 0.51 ($P = 0.0003$), while the R^2s of the other PCs were insignificant (PC1: 0.02, PC2: 0.01, PC4: 0.008). As described below (Fig. 3), such results were quite consistent across the eight animals used for this study.

Higher numbered components encoded information on statistical outliers which here tend to reflect higher spatial frequencies. For example, PC4 differentiated between neurons with RFs in the caudal D row vs E row. PC6 differentiated between neurons with RFs in the rostral whisker pad. Finally, PC5 positively weighted the neurons without RFs. PC5 also negatively weighted neurons with RFs centered on whiskers E2 and D6. This seemingly unlikely combination is reminiscent of our previously reported finding (Nicolelis et al., 1993, 1995) that many neurons which respond at short latency (4–10 ms) to stimulation of caudal whiskers (e.g. E2) often respond at longer latency (15–25 ms) to stimulation of the rostral-most whiskers (e.g. D6). Thus, the higher numbered principal components have successively more complex weighting patterns, whose functional significance is less clearly related to absolute RF position.

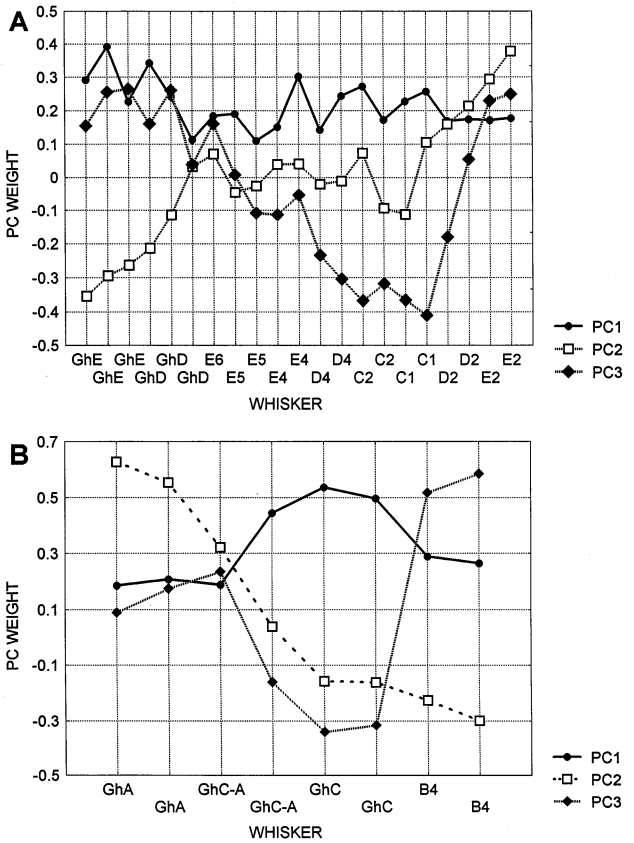

Fig. 3. Weighting coefficients of principal components derived from VPM neuronal ensembles recorded in additional animals. All were constructed using the same technique as in Fig. 5: Correlation matrices were constructed from neural activity measured during all 10-ms time intervals in long periods of spontaneous exploratory whisking behavior. RF locations were determined from quantitative RF mapping experiments carried out just after the spontaneous behaviors. Graphs depict the weighting coefficients in PC1–3 ('PC WEIGHT' on *Y*-axis) for each of the neurons, which are rank ordered along the *X*-axis according to rostrocaudal location of their RF centers ('WHISKER'). (A) Three line plots depict weighting coefficients of PC1–3, obtained from a PCA carried out on data from 21 VPM neurons simultaneously recorded during an 1545.43 s sequence of spontaneous exploratory whisking behavior in an awake rat. The RF centers of these 21 neurons ranged from the guard hairs just rostral to rows E and D ('GhE' and 'GhD') to the caudal large whiskers in the C, D, and E rows. When these were rank ordered according to rostrocaudal position, the PC2 weights reveal a roughly linear progression wherein the neurons with rostral RFs (GhE) are most negatively weighted, while those with caudal RFs (E2) are most positively weighted. PC3 weights neurons according to the dorsoventral position of their RFs: those with dorsal RFs (on the C1 and C2 whiskers) are most negatively weighted, while those with ventral RFs (E-row) are most positively weighted. (B) Similar line plots depict PCs 1–3 derived from eight VPM neurons in another rat, simultaneously recorded during 1812.965 s of spontaneous exploratory whisking behavior. The neuronal weightings in PC2 defined a roughly rostrocaudal gradient, most positively weighting the guard hairs rostral to the A-row (GhA), and most negatively weighting the B4 whisker. PC3 roughly defined a dorsoventral gradient, with most negative weightings on neurons with RFs on the guard hairs rostral to the C-row, and neutral weightings on neurons with larger fields which cover both GhC and GhA (GhC-A).

3.6. PCA results are similar even when derived in different conditions

Additional evidence for the high statistical reliability of these components is provided by the observation that the components changed only slightly when calculated from repeated experiments on the same neuronal ensembles. As is illustrated in Fig. 2A,B, this consistency in PCs was observed even when different time bins were used (10 ms in Fig. 2B vs 25 ms in Fig. 2A). In Fig. 2B the neuronal weights are rank ordered exactly as in Fig. 2A, revealing remarkably similar overall weighting patterns: PC2 is virtually the same in Fig. 2A,B, except that its polarity is reversed (insignificant in PCA). PC3 in Fig. 2A is equivalent to PC4 in Fig. 2B, although their polarities are reversed. This reversal of PCs 3 and 4 suggests a relatively slow time course of interactions between neurons with dorsal vs ventrally located RFs.

The weightings in Fig. 2C were remarkably similar to those in Fig. 2B, even though the PCs in Fig. 2C were derived from recordings of the same neurons obtained 40 min later during an experiment in which the E2 whisker was repetitively stimulated during periods of behavioral immobility (comprising about 80% of total experimental time). The only major difference between PCs 1–3 in these experiments is that PC3 in Fig. 2C reveals a relatively greater weighting of whisker E2, which was selectively stimulated during this experiment. The higher numbered components also exhibited remarkable equivalences, though altered in polarity and eigenvalue: PC5 in Fig. 2B,C is similar in weighting pattern, though reversed in polarity. Moreover, both are similar to PC6 in Fig. 2A. Finally, PC6 in Fig. 2A and PC5 in Fig. 2B,C contain similar weightings of the neurons on the left side of the figure (i.e. C5–D6 through D4).

To conclude, the basic weighting structure of the PCs derived from this neuronal ensemble remained remarkably constant over experimental time and over changes in bin size and behavior (e.g. spontaneous active whisking vs passive whisker stimulation). The proportions of time spent during these different behaviors were reflected more in the PC eigenvalues (and therefore the ordering of PCs) than in the PC weightings. Furthermore, the remarkable similarities between the components in Fig. 2B,C (which both use 10-ms bins) demonstrates a high level of statistical reliability of these calculations, even when relatively small data sets were used (Fig. 2C was derived using a 550 s experiment, vs 1821 s in Fig. 2A,B).

3.7. Statistical significance of PCs

The statistical significance of PCs can be assessed through calculation of S.E. of the eigenvalues and

weights (see Section 2). For the components in Fig. 2A, the average weighting coefficient in PC1 was calculated to be 12.98 times its S.E., and for the combined PCs 1–6 was 13.44 times the S.E. Moreover, only weights which were very close to zero were less than three times their S.E. Thus, the weights with low statistical significance had negligible impact on the components overall.

The S.E. of the eigenvalues, which specify the variance associated with each component, also tended to be very small fractions of their values. For example, the eigenvalue of PC1 in Fig. 2A was 4.26 ± 0.022 S.E., meaning that it explained a variance equivalent to 4.26 of the original neurons (18.5% of the total; each neuron explains a standardized variance of 1.0). Though for typical implementations of PCA this is not a particularly high eigenvalue, it is quite remarkable considering the complexity of the information carried within the discharge of 23 highly stochastic neurons during free behavior. We observed that PC1's eigenvalue increased to 14.56 when the time integral was raised to 500 ms, suggesting that much of the complex information and/or noise in this ensemble was expressed over shorter time periods.

3.8. Comparability of PCA results across animals

Similar results were obtained when PCA was used to analyze data from VPM neuronal ensembles in the seven other animals, two of which are shown in Fig. 3A,B. Though the neurons recorded in each animal had different RF mappings and discharge characteristics, and a range of time integrals (5–25 ms) were used, they tended to produce similar weighting patterns in their PCs. In all animals, PC1 contained roughly homogeneous positive neuronal weightings, and PC2 and, to a lesser extent, PC3 roughly encoded the position of RF centers according to particular gradients across the whisker pad. In Fig. 3A, for example, PC1 has relatively homogeneous weightings, but PC2 differentiates neurons with far rostral vs far caudal RFs. In contrast, PC3 sharply discriminates between neurons with RFs on row C vs row E. Using the regression analysis described above for Fig. 3A, the PC2s of five or the total eight animals were found to significantly ($P \ll 0.01$) encode rostrocaudal position. In four of eight of these animals the PC3s also significantly encoded dorsoventral position of neuronal RFs. Furthermore, the PCs in Fig. 3B showed a variant of this relationship: PC2 most selectively encoded the dorsoventral position ($R^2 = 0.60$, $P = 0.02$), while both PC1 ($R^2 = 0.70$) and PC2 ($R^2 = 0.64$) encoded rostrocaudal position ($P = 0.01$ for both). In none of the other seven animals did PC1, PC4 or PC5 yield any significant encodings of overall rostrocaudal or dorsoventral gradients. These statistics, therefore, support the general conclusions that: (1) PC1 generally contains roughly homogeneous positive neuronal weightings, (2) PC2 generally encodes the rostrocaudal position of RF centers across the whisker pad, (3) PC3 may encode overall dorsoventral position, (4) higher numbered PCs tend to encode more fine-grain spatial relationships, often defining sharp boundaries between adjacent whiskers or whisker groups.

These overall results were obtained despite the wide range in ensemble size and RF distribution. For example, the ensemble used for the PCs in Fig. 3A included 21 neurons, and that for Fig. 6B had eight neurons. Whereas the RFs in Fig. 3A covered the whole rostrocaudal extent of the whisker field, those in Fig. 3B covered a more limited area, mainly including the rostral whiskers and guard hairs. As such, PC2 and PC3 in Fig. 3B defined dorsoventral and rostrocaudal gradients across the rostral face, rather than across the whole whisker field. Thus, despite the obvious disadvantages associated with use of relatively small inhomogeneous data sets (as in Fig. 3B), the present results reveal a remarkably robust general tendency for successive PCs to encode sensory information in the form of successively finer spatial resolutions.

This correlation of PCs with spatial frequency bands corresponds closely to the components which we have derived using data from computer simulated sensory systems (unpublished observations) in which a model receptor sheet was activated with moving stimuli. This is remarkable considering that the PCs here were derived from VPM neuronal ensembles which received no sensory stimulation other than that produced by the animal itself during the normal course of spontaneous behavior.

3.9. Single neurons contribute variance to multiple coding dimensions

By definition PCs, such as those shown in Figs. 2 and 3, are othogonal and therefore define mappings in different dimensions. The fact that at least the first 3–6 PCs were found to exhibit distinct and consistent functional topographies suggests that these PCs may describe real dimensions of information processing. If so, each neuron may be considered to contribute a portion of its variance to several of these dimensions, as statistically measured by the square of its PC weighting (see Section 2). These weights, therefore, offer methods for defining each neuron's role in multiple dimensions of processing, and for mapping the variance weighted configuration of the neuronal ensemble involved in each of these functional tasks.

Fig. 4, for example, depicts the position of each neuron in Fig. 2A as a point in a space defined by PC1 and PC2 (Fig. 4A) and by PC3 and PC4 (Fig. 4B). Each neuron is labeled according to its principal whisker, as depicted in Fig. 2A. For illustration, consider the three neuron pairs whose principal whiskers are C2, D2 and E2. In PCs 1 and 2 (Fig. 4A) they are

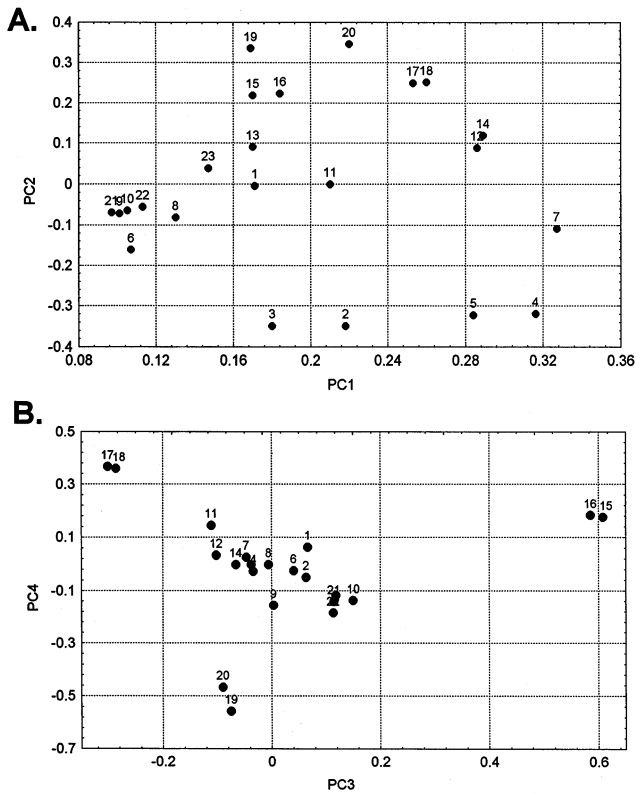

Fig. 4. Use of PCA to define functional relationships between neurons. (A) Neurons 1–23 (from Fig. 2A) plotted as dots according to their weightings in PC1 and PC2. (B) Neurons 1–23 plotted according to their weightings in PC3 and PC4.

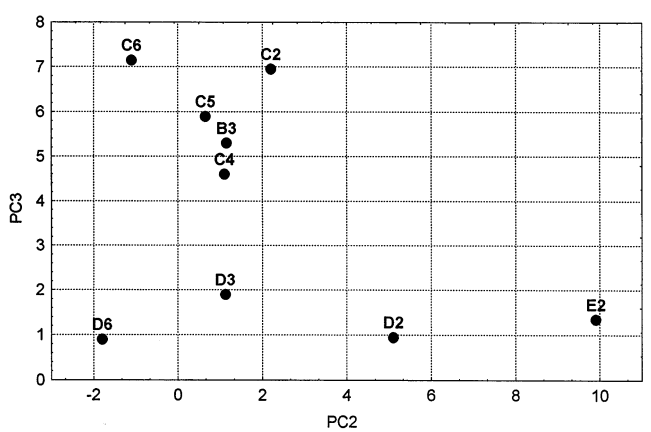

Fig. 5. Plotting neuronal population responses to whisker stimulation in a PCA-defined space reveals spatial arrangement of whiskers. Neuronal population responses to deflection of each of nine different stimulated whiskers were plotted within a space defined by PCs 2 and 3 (each dot representing the averaged responses to 300–600 deflections of the indicated whisker). The responses were measured during the peak short latency response period, i.e. between 5 and 8 ms post-stimulus (as shown in B and C). The arrangement of dots on this plot is generally consistent with the spatial arrangement of the indicated whiskers on the face.

part of two continuums, hypothesized to encode magnitude and rostrocaudal position, respectively. Each of these six neurons contributes 3–14% of the total variance to each of these encodings. In PCs 3 and 4 (Fig. 4B) they play a very different role, defining a 2D space in which objective spatial position appears to be much less important than high-contrast differentiation between the three whiskers (C2, D2 and E2). Each of the six neurons contributes a high percentage of its variance to this task (up to 36% for C2's weighting of PC3). Similarly selective differentiations of caudal whiskers were also observed in other animals used in this study. This selectivity may be explained by the fact that rats tend to employ their relatively short rostral whiskers as a group to touch objects during exploration, while their caudal whiskers project at widely different angles into space.

The present results suggest that the optimal mapping of afferent information by PCA (and the brain itself) may extract multiple different significant features of the sensory experience, using relatively small portions of each neuron's variance to generalize to global objective mappings of space or magnitude. Meanwhile, more local and selective dimensions of information processing consume larger amounts of variance from small subsets of neurons.

3.10. PCs classify neuronal population responses to stimulation of specific whiskers

The PCs derived here were found to be very effective tools for classifying sensory responses. In particular, PC2 and PC3 provided a highly efficient 2D subspace for clustering the neuronal population responses to discrete stimulation of different whiskers. To demonstrate, Fig. 5 shows a 'mapping' of each of the nine whiskers stimulated in this experiment into a space defined by PCs 2 and 3. The x or y coordinates of each point on this graph were defined by calculating eigenfunctions (see Section 2) for both PC2 and PC3 for stimulation of each of these nine whiskers. Here, eigenfunctions 2 and 3 were each calculated as the sums, weighted respectively by PCs 2 and 3, of the spiking responses (in the 4- to 8-ms latency epoch) of all 23 neurons to 300–600 stimulations of the indicated whisker. The resulting scatterplot shows existence of a unique, anatomically appropriate position for each whisker, especially in the rostrocaudal dimension. Moreover, it accurately plotted the positions of whiskers which were not within the center-RFs of any neurons within the sample, but were within the surround-RFs of some neurons (e.g. whiskers C4–6 and B3). These results therefore show that PCs derived from activity of a relatively small and biased sample of VPM neurons can effectively represent the spatial positions of a range of whisker stimulus positions. It is important to note, however, that this map does not reproduce the absolute X–Y positioning of the whiskers on the face.

Instead it provides a functional mapping of these whiskers, as defined by the response patterns of this set of neurons in the VPM occurring during spontaneous behavior.

Roughly similar whisker mappings were found in the eigenfunction 2–3 data from six of the other seven animals. Though these mappings were somewhat biased by the particular selection of neurons in each data base, the caudo-ventral whiskers tended to occupy larger areas of these maps than the dorsal or rostral whiskers. This is, of course, consistent with the anatomical mapping of these whiskers in the somatosensory system (Chapin and Lin, 1984). To conclude, this demonstration argues that population covariance patterns, even that occurring during general spontaneous behavior, contain a significant amount of information on the mapping of whisker location within a generalized 2D space. This space, however, is not an accurate objective map of the whiskers, or even their receptor densities, but is warped according to the patterns of temporal correlation between different whisker inputs. Finally, the proportion of population variance dedicated to this mapping is relatively small, in this case about 12% of the total (as calculated from eigenvalues in Fig. 2A).

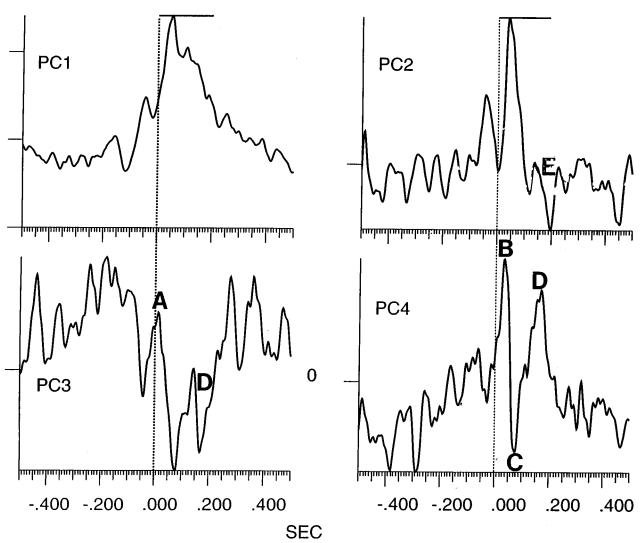

Fig. 6. Higher numbered PCs encode higher frequency domains of neuronal population responses to moving whisker stimuli. Peri-stimulus responses of PCs 1–4 to moving a probe across the mystacial whiskers. Each trace is the average of the indicated PCs over 17 trials. Initial contact of the probe on the caudal whiskers is indicated by vertical dotted lines. Brushing consisted of slowly moving a hand held cotton probe tip across the whiskers in alternate directions along an oblique caudo-dorsal to rostro-ventral axis. The bar above the traces indicates the approximate timing of the probe sweep in the rostro-ventral direction. Vertical axes depict average equivalent discharge rates of eigenfunctions: small ticks, 10 Hz. Horizontal axis depicts time (s) before and after the stimulus onset. See text for explanation of PC responses.

3.11. Feature detection by principal components

The above results also showed that the PCs may be used, in conjunction with data from simultaneously recorded neuronal populations, to construct feature detectors (i.e. eigenfunctions) whose general functional effectiveness far surpasses data measured from any single neuron. The following figures demonstrate that the eigenfunctions derived from the PCs in Fig. 2A are useful for detection of important events during ongoing behavior, not only when applied to multi-trial averaged data, but also to single trial (continuous) data.

The first question was whether eigenfunctions can be used to estimate the magnitude, velocity or direction of stimulus movement across the whiskers. Temporal patterns of activity of the eigenfunctions were observed to depict important features of stimulus movement, even though this study used only spatially related variables. (Neuronal activity was correlated only within the same time bins.) For example, the peri-event histograms in Fig. 6 show the averaged temporal responses of eigenfunctions 1–4 (from the PCs in Fig. 2A) to 17 brushings of a bar in a dorsocaudal-to-ventrorostral direction across the whiskers in an awake, immobile rat. The probe's successive contact with different whisker groups (as observed in frame-by-frame video analysis) is apparent in the responses of the various eigenfunctions: the caudal C-row whiskers were touched first, which produced peak 'A' in eigenfunction 3. (PC3 has highly positive weightings for neurons with RFs centered on whisker C2.) The probe then touched the caudal D-row whiskers, producing peak 'B' in eigenfunction 4. (PC4 positively weights the caudal D-row.) The probe then touched the caudal E-row whiskers, which through their negative weightings in PC3 and PC4, produced the valleys after 'A' in eigenfunction 3, and at 'C' in eigenfunction 4. The peaks following the valleys in eigenfunction 3 and eigenfunction 4 (around 'D') were mainly caused by 'bouncing back' of the caudal whiskers previously bent forward by the probe. Over the same time period (from 'A' to 'C') eigenfunction 2 exhibits a broader peak which declines slowly toward a deep valley at 'E'. This is explained by the fact that PC2 weights the caudal whiskers positively and the rostral whiskers negatively. Finally, eigenfunction 1, which positively weights all neurons, regardless of their whisker RFs, exhibits a peak which covers, and reflects the overall intensity of, the entire probing movement.

The above results demonstrate how the eigenfunctions can be used to process time-varying sensory input information by dividing it into ever finer spatiotemporal frequency domains. When a sensory surface interacts with a moving stimulus, its spatial frequencies are revealed as temporal frequencies. Here, successive PCs were associated with decreasing peak-to-valley durations of their sensory responses to the moving stimulus:

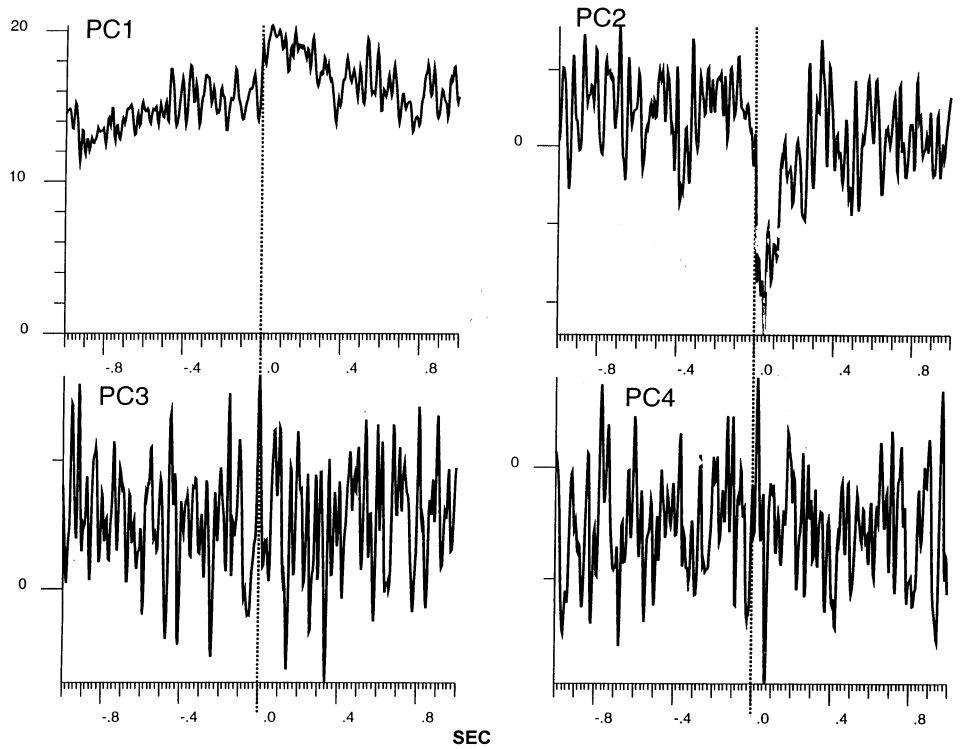

Fig. 7. PC2 selectively detects tactile contact on rostral whiskers. Peri-event averages of PCs 1–4 centered around the onset of 23 time periods when the rat contacted objects with the rostral mystacial whiskers. All these behavioral events were detected using frame-by-frame analysis of videotapes which were synchronized with data collection during the experiment. This further demonstrates PC2 codes (with negative polarity) for tactile exploration with the rostral whiskers. *X*-axes: pre- and post-touch time (s). Bins, 4 ms; small ticks: 20 ms. *Y*-axes: average equivalent firing rate, as in fig. 11. Small ticks: 1.0 spike/s.

$\sim$300 ms for PC1, $\sim$150 ms for PC2, $\sim$70 ms for PC3, and $\sim$35 ms for PC4. This combination of different spatial frequencies should optimally describe the linearizable information carried as covarying activity in this recorded neuronal population.

3.12. Principal component eigenfunctions resolve spatiotemporal patterns of whisker contact during exploratory whisking

Normally, rats obtain sensory information from their vibrissae through active whisking behavior. One of the critical applications of the eigenfunctions derived here was for the detection of particular active whisker movements across objects in the environment. This allowed a comparison of the sensory information obtained during whisker exploration, as opposed to passive stimulation with a probe.

In all eight animals used here, PCs 1–4 were consistently found to detect significant features of tactile contact on objects during tactile whisking. To demonstrate the typical robustness of these responses, Fig. 7 shows averages of the same eigenfunctions 1–4 centered around 23 instances of active exploratory contact of the rostral whiskers against objects (times determined by frame-by-frame video analysis). Though eigenfunction 2 exhibits a consistent and highly significant negative response during such behaviors, the responses of eigenfunctions 3 and 4, which mainly encode the caudal whiskers, show no significant responses. Finally, eigenfunction 1 exhibits a response pattern which is consistent with the generally increased whisker contact surrounding these behaviors. Similar peri-event averages of eigenfunctions were used to verify that the behavioral correlates of the above PCs depicted in Fig. 7, and equivalent analyses of data from the other seven animals, were consistent throughout the entire duration of the experiment.

Eigenfunctions, especially those constructed using populations of 20 or more neurons, were easily capable of detecting significant behavioral events on a single-trial, real-time basis. For illustration, Fig. 8 shows the same eigenfunctions 1–4 over a 20-s period of spontaneous behavior. Video analysis showed that this particular sequence was of interest because it consisted of a series of active head movements which brought the mystacial whiskers into contact with a Plexiglas wall just to the right of the animal. This allowed an analysis of the responses of the 23 neurons in the VPM to active movement of the whiskers in various directions across a smooth, flat tactile object. Particular tactile movements observed in frame-by-frame video analyses were repre-

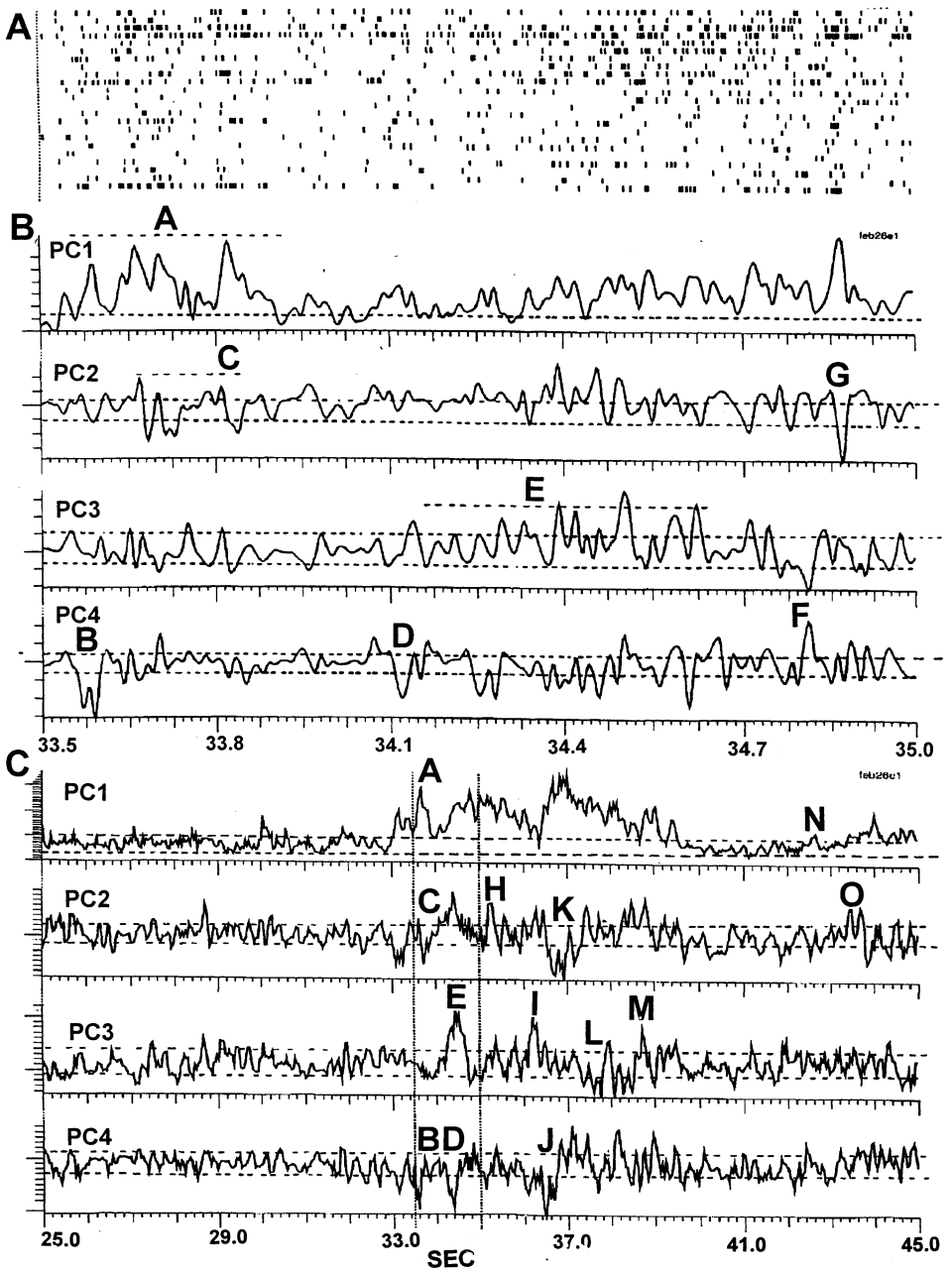

Fig. 8. Population vectors define timing and direction of tactile whisker contact. (A) Rasters of spiking activity of 23 simultaneously recorded neurons over a 1.5-s period. (B) Stripcharts of continuous eigenfunctions of PCs 1–4 over the same period during which the rat moved its whiskers in various directions against a wall. Letters A–G represent different movements of mystacial whiskers against a wall (see text), as observed in frame-by-frame analysis of videotape records synchronized to data collection in this experiment. (C) Activity of the same PC's over a 20-s period. Sequence B is contained between the vertical lines. *X*-Axis shows the absolute time (s) in the experiment for all recordings: Bins, 40 ms; small ticks, 200 ms. *Y*-Axes show equivalent 'firing rates' of the standardized weight-summed eigenfunctions: small ticks, 10 spikes/s. Horizontal lines through the eigenfunctions indicate 2.0 S.D. away from the mean spontaneous activity, as calculated during quiet resting behavior (each S.D. is 13.2 S.E.). Dotted line under A is 12 S.D.s above the mean; dotted lines under C and E are six S.D.s above the mean. Eigenfunctions were calculated as in Section 2 using 10-ms time integrals, and then smoothed into bins by averaging within a three-bin moving window.

sented in the eigenfunctions as peaks or valleys which were clearly distinguished from their 'background' activity. In Fig. 8B, C, the statistical significance of these peaks and valleys can be discerned by their relation to the confidence limits shown as horizontal dotted lines on each trace, defining eigenfunction activity levels two standard deviations (S.D.s) in either direction from the means, as measured during periods of pure resting behavior in the same experiment.

The sequence in Fig. 8B, as demarcated by vertical dotted lines in Fig. 8C involved the following specific movements of whiskers against the tactile surface, associated with peaks and valleys in various eigenfunctions: The peak at 'A' in PC1 represents the relatively nonselective global ensemble response to a sequence of active head and whisker movements commencing with a sudden head movement to the right and then down, sweeping the whiskers first in a backward and then downward direction against the wall. Statistically, this sequence in the eigenfunction 1 is highly significant, reaching up to 12 S.D.s from mean.

The higher numbered eigenfunctions also exhibit significant peaks which are more selective for particular parts of this behavioral sequence. For example, at the onset of rightward head turning eigenfunction 4 (PC4) exhibits a highly significant (10 S.D.s from the mean) negative deflection ('B' in Fig. 8B, C). This was produced by the downward and backward movement of the ventral whiskers against the wall, preferentially stimulating the caudal E-row whiskers. This negative deflection was predictable based on the pattern of weighting coefficients for PC4, which were highly negative for the two neurons with RFs on whisker E2. This response, however, was not simply formed by the spurious spiking of two single neurons. PC4 also negatively weighted two neurons with RFs on D4 and three neurons with no RFs. Examination of the raw spiking data for the total seven neurons with negative weightings for PC4 showed that five exhibited increased spiking during the negative deflection shown at B. Furthermore, the five neurons with strongly positive weightings in PC4 (>0.1) all exhibited decreased discharge during this same period. Thus, even this relatively small deflection of an eigenfunction for a high numbered component represents the highly significant joint activity of a neuronal subpopulation. Similar whisker movements against the wall were associated with other negative deflections of eigenfunction 4, such as at D and J in Fig. 8B, C.

PC2, which negatively weights rostral whiskers and positively weights caudal whiskers, was active during normal exploratory whisker movements in which the whiskers moved across objects in a rostral-to-caudal direction. An example is seen in PC2 in Fig. 8B, C in which the rostral-to-caudal succession of whisker contacts is reflected as negative-to-positive progression shown under 'C'. In other cases, such as in 'K', the rostral whiskers alone were used to explore objects on the floor, producing a pronounced depression in eigenfunction 2. Positive deflections of the eigenfunction 2 also carry important information consistent with its positive weighting of the caudal whiskers: the peak at 'H' in Fig. 8C depicts a right turn of the head which moved the caudal whiskers in a backward direction against the wall. Overall, these results demonstrate that PC2 encodes the direction of whisker sweeping across objects in the rostrocaudal axis. Similarly, eigenfunction 3, whose PC(3) positively weights neurons with RFs in the more dorsal whiskers (rows B and C), was most active during movements in the dorsoventral direction. As an example, 'E' shows the response of eigenfunction 3 to dorsalward movements of the whiskers against the wall. Similar, but shorter movements occurred at 'I', 'L' and 'M'.

3.13. Eigenfunctions reveal global and local neural ensemble information in continuous time

Eigenfunctions were also employed here to depict neural ensemble information in stripcharts, which allowed visualization of the state of multiple eigenfunctions in continuous time. These depicted the moment-to-moment status of multiple dimensions of population information which could never be observed in analyses at the single neuron level. For example, the eigenfunction stripcharts in Fig. 8 reveal the presence and time course of distinct spontaneous oscillatory phenomena. The onset and offset timing of these rhythms could not be detected in peri-event averages, but instead required continuous-time depiction of the state of the neuronal ensemble. We have observed these 8–12 Hz oscillations in the PC1s of neuronal ensembles in the somatosensory thalamus or cortex in all of the 20 animals recorded for this study, and have routinely utilized this ability of eigenfunction 1 to depict such oscillatory phenomena in real time and to carry out precise analyses of their functional characteristics (Nicolelis et al., 1995). Video analyses (see Section 2) showed that these oscillations characteristically began during the period of attentive immobility which just precedes active whisker twitching, and continue until onset of larger active exploratory movement. They appear, therefore, to represent a global neurophysiological process which pervades the sensorimotor thalamocortical system during behavioral preparation for movement.

Whereas eigenfunction 1 typically reveals major global phenomena such as spontaneous global oscillations, the higher numbered components typically code for more 'local' information. To illustrate further, Fig. 9 shows a raster (A) of the simultaneous activity of these 23 cells plus PCs 1 and 2 (B) over a 1.4-s period during which the E2 whisker was subject to a single (3°;

at 'S') mechanical displacement. While eigenfunction 1 again clearly reveals the global 8–12 Hz oscillations, the higher numbered eigenfunctions follow them only weakly. Instead, eigenfunctions 2–4 exhibit selective responses to the E2 whisker stimulation (S) which are clearly differentiated from the oscillatory peak (O) that appears slightly later.

The mechanism by which the eigenfunctions can selectively filter different dimensions of global and local information in neuronal ensembles involves the use of positive and negative neuronal weightings to selectively 'subtract' the information already encoded by lower numbered components. Since PC1 normally has a relatively homogeneous set of exclusively positive weightings, it identifies 'global' functions, such as the 8–12 Hz oscillations, which are characteristic of nearly all neurons in the ensemble. These typically constitute the greatest source of variance in eigenfunction 1, but are effectively cancelled out in the higher numbered components. Thus, the orthogonalization of network covariance by PCA effectively differentiates between global and local sources of neural information.

At time 'S' in Fig. 9B, local information is presented in the form of a sensory stimulus which differentially affects the neurons in the ensemble. The responses of the different eigenfunctions to this stimulus can be predicted by their weightings of neurons with RFs centered on the stimulated whisker (E2) and its neighbors (e.g. D2, D4 and C2) all of which respond at some level to E2 stimulation. Whereas PC2 weights E2 and these neighbors negatively, PC3 and PC4 selectively weight E2 positively, but some of its neighbors negatively. Because of the fact that whisker E2 was stimulated alone, and not in conjunction with its neighbors, eigenfunction 2 produced a cleaner resolution of the stimulus than did eigenfunction 3 or eigenfunction 4. Finally, the eigenfunction for PC5, which has near zero weightings for all neurons with RFs around whisker E2, exhibited no response to this stimulus.

The response selectivity of eigenfunctions 2–4 to whisker E2 stimulation was verified in peri-stimulus averages (Fig. 9C). Whereas the whisker stimulation increased the magnitude of the average eigenfunction 1 equivalent 'discharge rate' from a mean 8.2 to maximum 15.7 Hz after the stimulus, for a signal/background (S/B) ratio of 1.93, the activity of PC2 increased (with negative polarity) from a mean -0.3 to -5.9 Hz after the stimulus, for a S/B ratio of 18.9. Even when the high background activity of eigenfunction 1 is disregarded by calculating the responses in terms of deviation from the mean, its maximal response to whisker E2 stimulation was only 15.2 S.D.s from the pre-stimulus mean, compared with 24.0 S.D.s for PC2, 14.5 S.D.s for PC3 and 22.9 S.D.s for PC4. This greater resolution of E2 whisker stimulation by PC2 is more remarkable when one considers that the higher numbered components by rule explain much less total statistical variance than PC1. Here, the eigenvalue for PC1 was 3.8, and for PC2, 1.5. Thus, PC2 devoted a much higher proportion of its total variance to E2 whisker responses than does PC1.

4. Discussion

4.1. PCs and multidimensionality

In this study, eigenvalue decomposition of neuronal ensemble activity in the VPM measured during spontaneous behavior yielded at least 3–6 uncorrelated factors (PCs) whose resolution of significant information in the ensemble (i.e. explained variance) was considerably greater than that of any single neuron. This finding appears to validate our hope that PCA could successfully provide an optimal linear representation of the 'signals' in these recordings, which are concentrated in the first few components, while filtering out 'noise' (mainly uncorrelated neuronal activity), which is sequestered in the remaining components. Because of the orthogonality criterion for PCs, each represented a separate 'dimension' of covariant activity in the ensemble. Moreover, each of these PCs was found to possess a clear and distinct functional attribute, suggesting that together they provide clues toward resolution of the fundamental axes around which the different dimensions of information processing might be carried out within the thalamocortical circuitry. These findings are consistent with the general framework of parallel distributed processing in neuronal networks (Rumelhart et al., 1986a): each processing task is distributed across the network, and each single constituent neuron is involved in processing multiple tasks. Here, the statistical contribution of each neuron's variance to a given processing dimension (i.e. PC) is quantitatively defined as the square of the weighting for that PC.

4.2. Functional attributes of PCs

The functional attributes of each PC were reflected both in its weightings of neurons with different receptive fields, and also the physiological properties of the population vectors derived from such weights. The finding that most of the derived eigenvectors defined a different 'topography': ranging from the highly generalized maps of the first few PCs, to the increasingly more selective mappings encoded by each subsequent PC. Although the sensory thalamus is commonly considered to contain a single receptor surface density map, PCA's optimal mapping of the linear subspaces embedded in actual VPM neuronal activity was unable to resolve all such neural information into such a single two-dimensional topographic representation. In fact, the greatest

single source of variance (i.e. PC1) was non-topographical, mainly encoding the magnitude of activity across the whole ensemble. In contrast, PC2 was typically topographical, but generalized it maximally across the neural population by encoding a linear rostrocaudal gradient. Subsequent PCs became ever more selective, often encoding sharp contrasts between adjacent whiskers, but also showing multiple peak/valley features within the same PC. The topographic specificity of this organization of PCs is remarkable considering that they could be derived using data obtained either during sensory stimulation or spontaneous behavior which included exploratory whisking. In fact, these behavioral differences more often produced changes in the eigenvalues than the PC weighting patterns, therefore changing their relative ordering. We conclude, therefore, that neural population activity in the VPM has an intrinsic and relatively invariant multidimen-

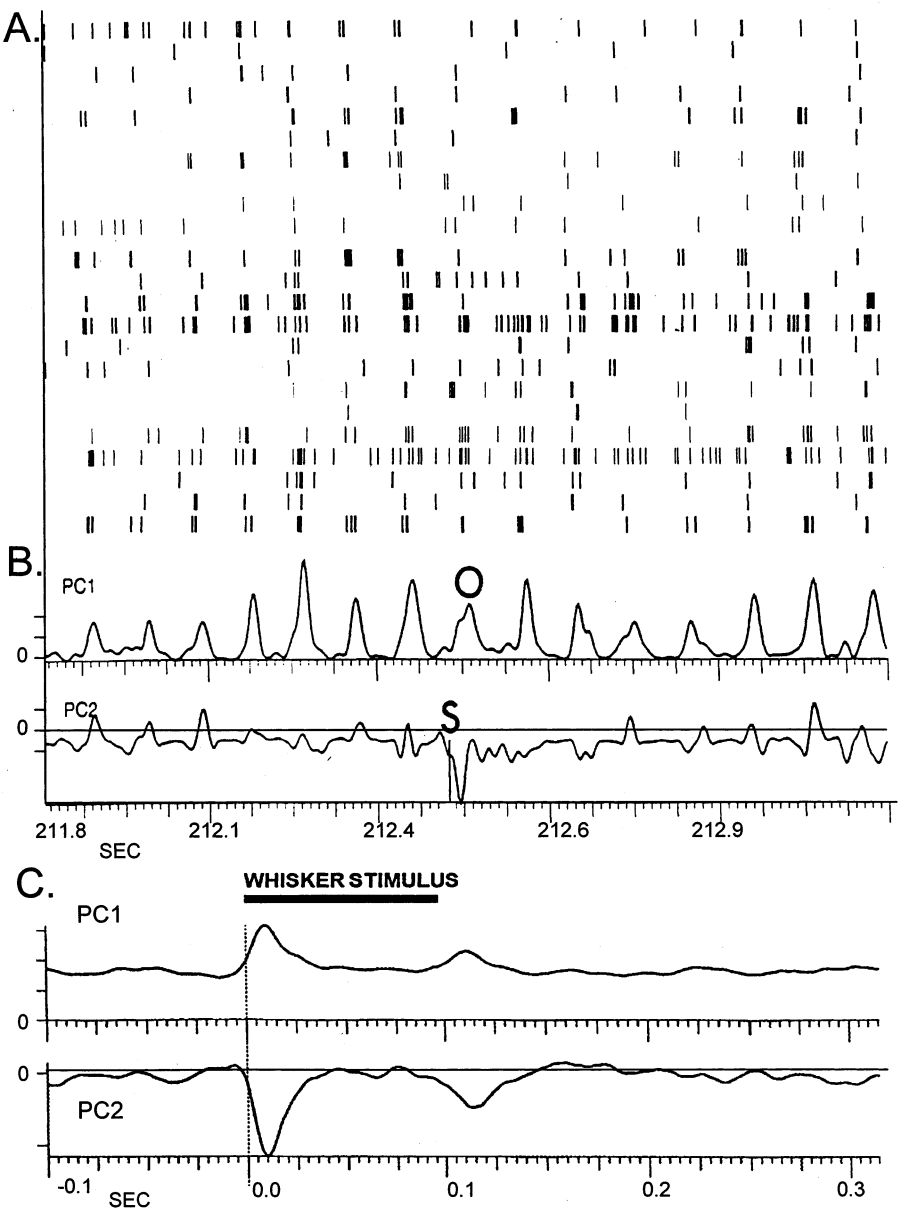

Fig. 9. PCs differentiate global from local information. In the VPM thalamus, spontaneous oscillations are 'global' in that most neurons are synchronized. In contrast, single whisker stimulation is local. (A) Spike rasters show activity of 23 simultaneous neurons over a 1.4-s period of an experiment involving intermittent E2 whisker stimulation, under awake conditions. (B) Eigenfunctions (PCs) 1 and 2 over this same time period. Eigenfunction 1 selectively indicates spontaneous global oscillatory peaks (e.g. at 'O'), while eigenfunction 2 selectively indicates response ('S') to stimulation of whisker E2. (C) Peri-event histograms showing averaged responses of eigenfunctions (PCs) 1 and 2 to 306 repetitions of such stimuli during the same experiment. Stimuli consisted of 3° step deflections of the E2 whisker (100-ms duration, as shown by bar above). Responses to both the onset and offset of the stimuli are seen in both eigenfunctions. Both (B) and (C): Vertical axes depict average equivalent discharge rates of eigenfunctions: ticks, 10 Hz. Horizontal axes depict time (s).

sional factor structure which is maintained across different waking behaviors. The behaviors themselves appear to be largely encodable as modifications in the relative variances (i.e. activity levels) allocated to the different dimensions.

4.3. Equivalent findings from computer simulations

Interestingly, we have obtained very similar results by performing PCA on data obtained from a computer model of a simple sensory system (unpublished data). In this, a layer of neurons is fed by partially overlapping inputs from a linear matrix of receptors which are activated by moving stimuli. The PCs were observed to define a sequence of increasing spatial frequencies across the receptor surface, going from a single positive bell-type curve (PC1), to a gradient/half sinusoid (PC2), a full sinusoid (PC3), and so on. This sequence was found to reverse when the configuration of neuronal inputs was changed from partial-shifted overlap to center-surround inhibition: the weighting pattern originally exhibited by PC1 (with the highest eigenvalue) became that exhibited by the last PC (with the lowest eigenvalue). Thus, the current findings argue that afferent responses in the VPM approximate a partial overlapping ('distributed') organization, rather than a center-surround ('local') organization. In the distributed-type organization, the highest eigenvalue components are constituted by small contributions of variance from large populations of neurons. Such components have the greatest opportunity to extract and generalize shared information across the ensemble.

4.4. PCA, Hebb-type learning, and thalamocortical representations

PCA's detection of such generalized information emerging from the population of recorded neurons may have major implications for understanding how sensory input is processed, not only in the VPM, and also in its major target, the SI cortex. In fact, the known equivalence between PCA and general Hebbian learning suggests that it may be an especially powerful and functionally relevant method for characterizing the structure of sensory representations in brain regions which utilize Hebb-like adaptation for establishment or reorganization of synaptic connections. It is intriguing, therefore, to compare the weighting patterns of these PCs with our previously published findings about the diversity of shapes and sizes of receptive fields (RFs) in the whisker area of the rat SI cortex (Chapin, 1986). Using quantitative measurements, such RFs were observed to vary in size from single whiskers to the whole whisker field. Moreover, many of the RFs showed pronounced excitatory/inhibitory gradients between adjacent whiskers, or showed multiple peaks separated by inhibitory troughs. These cortical RFs are surprisingly similar to the topographies expressed by the different PCs defined here in VPM neuronal ensembles. As such, they could be produced by (polysynaptic) patterns of thalamocortical input weightings roughly similar to those derived here using PCA. The development and maintenance of such weighting patterns could result from Hebb-like (PCA-like) activity dependent adjustments of synaptic strengths in the SI cortex.

4.5. Validity of PCA for understanding sensory representations

The above observations lend some validity to the notion that the codes derived here using PCA may have some relation to 'internal' codes, as expressed either across neural populations or even within certain single neurons. It is reasonable to suggest that neuronal ensemble outputs could make weighted synaptic contacts on downstream neurons, and that those weights could be modified and maintained according to their covariance patterns, as in PCA and Hebb-type learning. Those neurons or populations could then provide a real-time 'read out' of a given PC, similar to the eigenfunctions constructed here. A major issue, however, stems from the obvious fact that biological neurons have many nonlinear properties. To a certain extent, this is mitigated by our observation here that multi-spike train data from larger neural populations tend to converge on normal distributions from which linear approximations can be extracted. However, further progress may depend on improving our knowledge of the nonlinear aspects of the underlying information in these ensembles, and use of this knowledge to develop appropriate nonlinear PCA and PCA-like algorithms. Many such methods have been recently developed, especially in the field of artificial neural networks (Karhunen and Joutensalo, 1994). Unfortunately, the formal mathematical bases for nonlinear PCA is not yet sufficiently developed for it to be widely accepted in statistical analysis. For example, the major known advantage of nonlinear PCA appears to be its improved ability to separate independent signals from a noisy mixture (Karhunen and Joutensalo, 1994). Such a capability would have limited usefulness here: our aim is not to separate all of the individual signals impinging on a neuronal population, but to extract the informational features produced by the association of these signals.

4.6. Statistical resolution of PCA derived functions

The statistical resolution of functionally important information by these PCs was very high, as determined by a number of measures. First, the S.E.s of the PC weights and eigenvalues tended to be very small frac-

tions of the total values. Second, the responses of the derived eigenfunctions to functionally significant events tended to be many S.D.s away from baseline activity. From the current results it is clear that the statistical resolution and 'biasing' of the information derived using PCA is dependent on: (1) the total number of sampled neurons, (2) the time period over which they are recorded, (3) the size and complexity of the area sampled, and the homogeneity of sampling within that area, and (4) the sampling time integral, which collapses the temporal complexity of the spike train signals. Theoretically, if more neurons were recorded over longer time periods using shorter time integrals, more significant local informational factors could be pulled out of the noise.

One obvious distinction between the PCA approach used here and traditional PCA is that a relatively large number of components is needed to summarize most of the total variance. Here, only about 50% of the total variance was explained by the first 25% of the components. This fact, however, does not compromise PCA's usefulness as a technique for reducing the dimensionality of complex information sets. Instead, it demonstrates the predictable result that neural activity in the VPM is relatively complex and high dimensional during waking behaviors. One could easily reduce this complexity by integrating over longer time bins or by averaging the data over multiple repetitions of the exact same stimulus event, but this is not desirable when the ultimate aim is to resolve the general functional repertoire of this nucleus, with a fine spatial and temporal resolution. Moreover, since a relatively large proportion of the total variance of single neuron spiking is apparently 'noise' (i.e. is not shared with other recorded neurons) most of the total ensemble variance must inevitably be used to explain this noise. This fact underscores the importance of using PCA to concentrate 'signal' information in the lower numbered components, while consigning the noise to the higher numbered components.

4.7. Eigenfunctions

The above results demonstrate that a range of functionally significant neural information can be resolved through eigenfunctions constructed by using PCA to provide weightings for averaging the activity of simultaneously recorded neurons. In general, these provided a much greater resolution of neural events than could be obtained with data from any single neuron, and even greater resolution was obtained by combining multiple eigenfunctions. A major advantage of this increased resolution is that a number of significant sensory-behavioral events could be reliably detected on a single trial basis using stripcharts of one or several eigenfunctions. This alleviates the necessity of averaging neuronal activity over multiple trials.

An additional advantage is the ability of the PCA derived eigenfunctions to 'focus' on particular informational features embedded in neuronal ensembles. This represents a major improvement over the use of simple unweighted ensemble averages (Dormont et al., 1982), which are only effective for encoding one dimension of information. Thus, combining the information from eigenfunctions 2 and 3 improved the ability to classify neural responses to stimulation of different whiskers, in fact mapping the whiskers roughly according to their topographic location on the face. The selectivity provided by this multidimensional coding would not have been possible with the simple ensemble average.

This ability of eigenfunctions to resolve significant sensory information in real time was especially useful for analysis of neural ensemble activity during spontaneous behavior. In most cases, each of the first few eigenfunctions were robustly correlated with observable features of sensory-behavioral function, and these were predictable based on their PC weighting patterns. Thus, eigenfunction 1 tended to depict global, ensemble-wide functions, such as the overall magnitudes of sensory stimuli, regardless of their position or direction. In contrast, PCs 2 and 3 were more selective for whisker position, and more importantly, for specific directions of stimulus movement across the whisker field. Indeed, during whisking behavior these eigenfunctions tended to reveal the direction and speed of whisker movement across surfaces more than the identities of the specific whiskers which were touched. Finally, the higher numbered components tended to encode information in higher spatial frequency domains, but more importantly defined specific relationships between neurons representing particular nearby whiskers. To conclude, the eigenfunctions derived using PCA defined a functional topography between neurons. The degree to which this matched the anatomical topography between whiskers on the face was a function of the neural transformation of spatiotemporal patterns of whisker receptor activation during spontaneous whisking.

To a large extent, the lower numbered eigenfunctions express emergent, network-wide information, rather than information sequestered within small groups of neurons. Thus, these eigenfunctions allow measurement of information which exists mainly through small contributions of variance from each of a large number of neurons across the network. The resolution of such information is largely dependent on the number of neurons included in the population average. It can be predicted, therefore, that development of techniques for recording larger numbers of neurons in functional ensembles will allow increasingly fine resolution of the informational parameters involved in somatosensory processing.

The fact that the eigenfunctions here, which were constructed using relatively small neural ensembles (8–

24 neurons) were able to detect, on a trial-to-trial basis, a number of significant behavioral events suggests that it might soon be possible to move beyond the classical neurophysiological requirement for averaging multiple repetitions of a stimulus. This capability is important not just for reasons of efficiency, but also because it is virtually impossible to create perfectly reproducible conditions for serial testing of neuronal properties. Not only are the behavioral conditions impossible to reproduce, but internal brain states which cause distinctive patterns of temporal coherence between neurons are even less controllable. Thus, network-based approaches such as that explored here could help alleviate the classical dependence of behavioral neurophysiology on overtrained animals. This would allow investigators to more precisely define the optimal behavioral tuning of neural activity by allowing it to be correlated with a much wider range of spontaneous and trained behaviors. In other words, if the experiment focuses on a narrow set of parameters chosen by the investigator, it cannot claim to have found the optimal property of the neurona.

The ability to use PCA and/or other methods to encode multi-neuron population vectors marks an important development in that it is now possible to resolve behaviorally significant brain information on a single trial basis. The next step is to extract such brain information in realtime and manifest it electronically in the real world. As an example, we have recently shown that PCA can be used to encode a realtime readout of 32-neuron population activity recorded in the motor cortical forelimb area of rats trained in a lever positioning task (Chapin et al., 1999). These rats were able to utilize such electronically manifested cortical 'motor' signals to directly control movement of a robot arm. Because of the accuracy imparted by using large neuronal populations, the animals were able to move the robot arm to fetch water from a dropper, and return it to their mouths using brain activity alone.

4.8. PCA vs other strategies for depicting neuronal population information

PCA is but one of a number of techniques which could be used to characterize neuronal population information. Since PCA is primarily descriptive, it does not depend on any preconceived theory about coding in the ensemble. It is significant, therefore, that the eigenfunctions derived here tended to be clearly and consistently correlated with externally observable sensory or motor phenomena. Nevertheless, there is no rule that each eigenfunction must necessarily code for a single specific identifiable behavioral event. For example, eigenfunction 1 was found here to express overall magnitude of sensory stimulation, plus global 8–12 Hz oscillations during attentive immobility behaviors which were preparatory to onset of rhythmic whisker movement (Nicolelis et al., 1995). Thus, the covariance mappings provided by PCA constitute opportunities to observe the information provided by functional groupings not anticipated by the experimenter. In fact, any close matching between eigenfunctions and target behaviors must be regarded as fortuitous. Correlated discharge between neurons can be caused by many internal and external factors, and need not necessarily match an experimenter's pre-existing hypothesis about coding in the system. For this reason it may be useful to combine PCA with techniques optimally designed for classifying groups, such as discriminant analysis, classification and regression trees (CART; Breiman et al., 1984), or neural networks with weights defined through supervised learning techniques (Rumelhart et al., 1986b). This 'hypothesis free' aspect of the PCA is also different from population coding based on tuning functions (Georgopoulos et al., 1986, 1988, 1989).

Acknowledgements

This work was supported by NINDS grant NS-26722 and DARPA/ONR grant N00014-98-1-0679 to J.K. Chapin.

References

Baldi P, Hornik K. Neural networks and principal components analysis: Learning from examples without local minima. Neural Networks 1989;2:53–8.

Bourlard H, Kamp Y. Auto-association by multilayer perceptrons and singular value decomposition. Biol Cybern 1988;59:291–4.

Breiman L, Friedmaan J, Olshen R, Stone C. Classification and Regression Trees. Belmont, CA: Wadsworth, 1984.

Chapin JK. Laminar differences in sizes, shapes, and response profiles of cutaneous receptive fields in the rat SI cortex. Exp Brain Res 1986;62:549–59.

Chapin JK, Lin C-S. Mapping the body representation in the SI cortex of anesthetized and awake rats. J Comp Neurol 1984;229:199–213.

Chapin J, Nicolelis M, Yu C-H, Sollot S. Characterization of ensemble properties of simultaneously recorded neurons in somatosensory (SI) cortex. Abstr Soc Neurosci Annu Mtg 1989.

Chapin JK, Markowitz RA, Moxon KA, Nicolelis MAL. Direct real-time control of a robot arm using signals derived from neuronal population recordings in motor cortex. Nature Neurosci 1999;2:664–70.

Churchland PM. A neurocomputational perspective. Cambridge, MA: MIT Press, 1989.

Dormont JF, Schmied A, Condé H. Motor command in the ventrolateral thalamic nucleus: Neuronal variability can be overcome by ensemble average. Exp Brain Res 1982;48:315–22.

Erickson RP. Stimulus coding in topographic and nontopographic afferent modalities: on the significance of the activity of individual sensory neurons. Psychol Rev 1968;75(6):447–65.

Georgopoulos AP, Schwartz AB, Kettner RE. Neuronal population coding of movement direction. Science 1986;233(4771):1416–9.

Georgopoulos AP, Kettner RE, Schwartz AB. Primate motor cortex and free arm movements to visual targets in three-dimensional space. II. Coding of the direction of movement by a neuronal population. J Neurosci 1988;8(8):2928–37.

Georgopoulos AP, Lurito JT, Petrides M, Schwartz AB, Massey JT. Mental rotation of the neuronal population vector. Science 1989;243(4888):234–6.

Hertz J, Krogh A, Palmer RG. Introduction to the Theory of Neural Computation. Reading: Addison-Wesley, 1991.

Hrycej T. Supporting supervised learning by self-organization. Neurocomputing 1992;4:17–30.

Karhunen J, Joutensalo J. Representation and separation of signals using nonlinear PCA type learning. Neural Networks 1994;7:113–27.

Kjaer TW, Hertz JA, Richmond BJ. Decoding cortical neuronal signals: network models, information estimation and spatial tuning. J Comp Neurosci 1994;1:109–39.

Laubach M, Shuler M, Nicolelis MAL. Independent component analyses for quantifying neuronal ensemble interactions. J Neurosci Meth 1999;94:141–54.

McClurkin JW, Optican LM, Richmond BJ, Gawne TJ. Concurrent processing and complexity of temporally encoded neuronal messages in visual perception. Science 1991;253:675.

Nicolelis MAL, Chapin JK. The spatiotemporal structure of somatosensory responses of many-neuron ensembles in the rat ventral posterior medial nucleus of the thalamus. J Neurosci 1994;14(6):3511–32.

Nicolelis MAL, Lin C-S, Woodward DJ, Chapin JK. Distributed processing of somatic information by networks of thalamic cells induces time-dependent shifts of their receptive fields. Proc Natl Acad Sci 1993;90:2212–6.

Nicolelis MAL, Baccala LA, Lin RCS, Chapin JK. Sensorimotor encoding by synchronous neural ensemble activity at multiple levels of the somatosensory system. Science 1995;268:1353–8.

Oja E. A simplified neuron model as a principal component analyzer. J Math Biol 1982;15:267–73.

Oja E. Neural networks, principal components, and subspaces. Int J Neural Syst 1989;1:61–8.

Oja E. Principal components, minor components, and linear neural networks. Neural Networks 1992;5:927–35.

Rumelhart DE, McClelland, and the PDP Research Group. Parallel Distributed Processing: Explorations in the Microstructure of Cognition, Vol. 1. Cambridge, MA: MIT Press, 1986.

Rumelhart DE, Hinton GE, Williams RJ. Learning representations by back-propagating errors. Nature 1986b;323:533–6.

Sanger TD. Optimal unsupervised learning in a single-layer linear feedforward neural network. Neural Networks 1989;2:459–73.

Shin H-C, Chapin JK. Modulation of afferent transmission to single neurons in the ventroposterior thalamus during movement in rats. Neurosci Lett 1990;108:116–20.